crystals

MDPI

Correlation Between Structural and Transport Properties of Ca-Doped La Nickelates and their Electrochemical Performance

Elena Pikalova [1,2,*], Vladislav Sadykov [3,4], Ekaterina Sadovskaya [3], Nikita Eremeev [3], Alexander Kolchugin [1], Alexander Shmakov [3,5,6], Zakhar Vinokurov [3,5,6], Denis Mishchenko [3,4], Elena Filonova [2] and Vladimir Belyaev [3]

[1] Institute of High Temperature Electrochemistry UB RAS, 620066 Yekaterinburg, Russia; laba50@mail.ru
[2] Ural Federal University named after the First President of Russia B.N. Yeltsin, 620002 Ekaterinburg, Russia; elena.filonova@urfu.ru#
[3] Federal Research Center Boreskov Institute of Catalysis, 630090 Novosibirsk, Russia; sadykov@catalysis.ru (V.S.); sadovsk@catalysis.ru (E.S.); yeremeev21@gmail.com (N.E.); shurka@catalysis.ru (A.S.); vinzux@mail.ru (Z.V.); q14999@yandex.ru (D.M.); belyaev@catalysis.ru (V.B.)
[4] Department of Natural Sciences, Novosibirsk State University, 630090 Novosibirsk, Russia
[5] Budker Institute of Nuclear Physics SB RAS, 630090 Novosibirsk, Russia
[6] Department of Physics, Novosibirsk State University, 630090 Novosibirsk, Russia
* Correspondence: e.pikalova@list.ru

Supplementary Materials

Table S1. Final synthesis temperature of the $La_{2-x}Ca_xNiO_{4+\delta}$ samples, specific surface area of the powdered materials, determined by the BET method and theoretical density, calculated from the X-ray diffraction (XRD) data.

Sample	Composition	T_{sint} [°C]	S_{BET} [$m^2 g^{-1}$]	ρ_{XRD} [$g\ cm^{-3}$]
LNO	$La_2NiO_{4+\delta}$	1100	1.24	7.04
LCNO01	$La_{1.9}Ca_{0.1}NiO_{4+\delta}$	1100	1.30	6.85
LCNO02	$La_{1.8}Ca_{0.2}NiO_{4+\delta}$	1100	1.39	6.72
LCNO03	$La_{1.7}Ca_{0.3}NiO_{4+\delta}$	1100	1.63	6.60
LCNO04	$La_{1.6}Ca_{0.4}NiO_{4+\delta}$	1100	1.53	6.47

Table S2. Summary of bond-valence and global instability indexes (GII) for the $La_{2-x}Ca_xNiO_{4+\delta}$ samples calculated by Rietveld method from the HRD data.

		$x = 0.0$	$x = 0.1$	$x = 0.2$	$x = 0.3$	$x = 0.4$
Bond valence sum (BVS)	La^{+3}	2.58(1)	2.69(1)	3.003(2)	3.14(1)	3.523(3)
	Ca^{+2}	-	1.55(1)	1.725(1)	1.80(1)	2.024(2)
	$O1^{-2}$	2.137(1)	2.253(1)	2.421(1)	2.572(1)	2.768(1)
	$O2^{-2}$	1.61(1)	1.69(11)	1.778(2)	1.89(1)	1.987(2)
	Ni^{+2}	2.35(1)	2.47(1)	2.648(0)	2.75(1)	3.063(0)
Ni oxidation state		2.34(1)	2.32(1)	2.38(1)	2.40(1)	2.40(1)
Global instability index (GII)		0.34	0.37	0.38	0.44	0.63
GII [42]		0.2904	0.3162	0.3595	0.4952	-

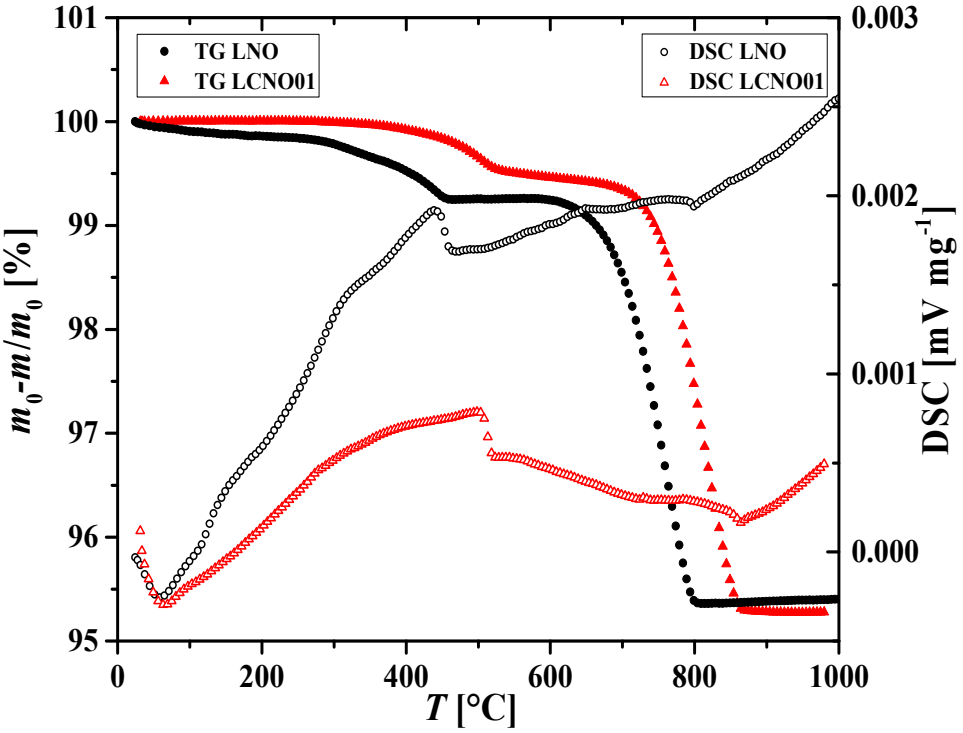

Figure S1. Temperature dependences of mass loss (TG) and differential scanning calorimetry (DSC) curves for $La_2NiO_{4+\delta}$ and $La_{1.9}Ca_{0.1}NiO_{4+\delta}$ samples in H_2-containing atmospheres.

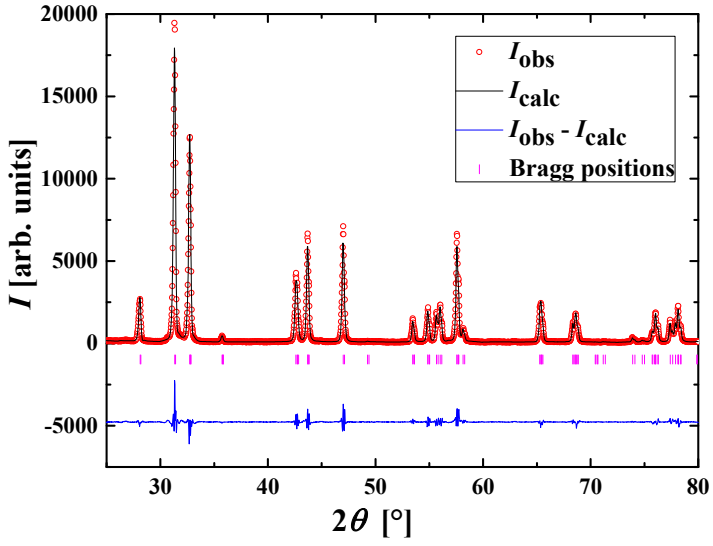

Figure S2. Experimental and calculated XRD patterns of the $La_2NiO_{4+\delta}$ sample.

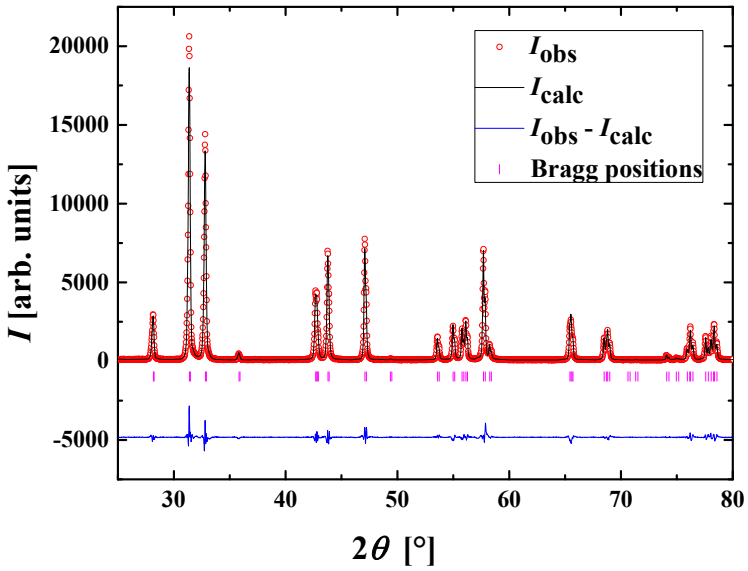

Figure S3. Experimental and calculated XRD patterns of the $La_{1.9}Ca_{0.1}NiO_{4+\delta}$ sample.

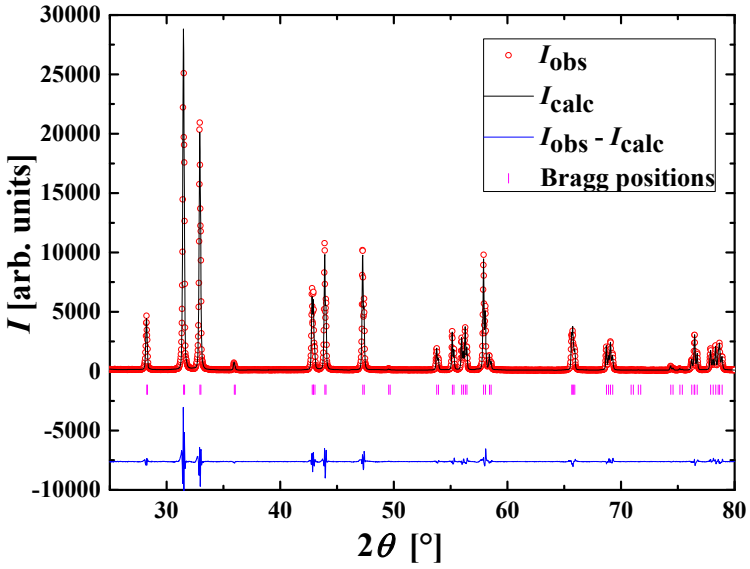

Figure S4. Experimental and calculated XRD patterns of the $La_{1.8}Ca_{0.2}NiO_{4+\delta}$ sample.

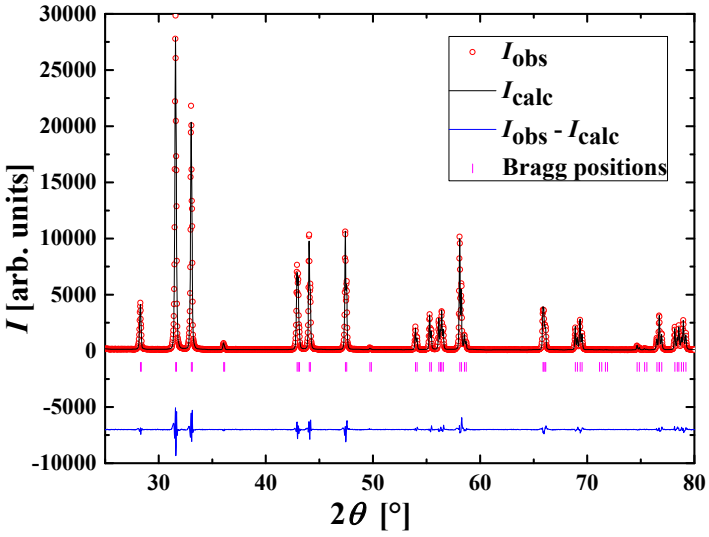

Figure S5. Experimental and calculated XRD patterns of the $La_{1.7}Ca_{0.3}NiO_{4+\delta}$ sample.

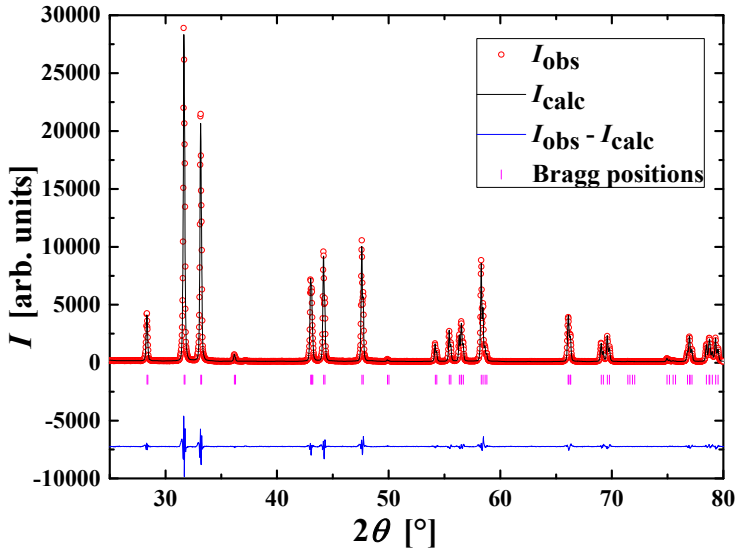

Figure S6. Experimental and calculated XRD patterns of the $La_{1.6}Ca_{0.4}NiO_{4+\delta}$ sample.

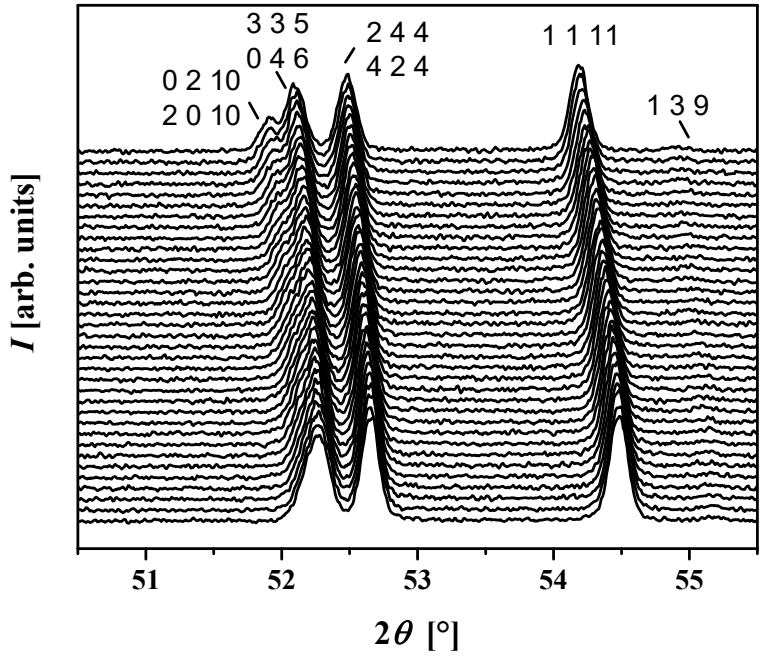

Figure S7. Experimental XRD patterns of the $La_2NiO_{4+\delta}$ sample obtained during heating in synthetic air up to 700°C with a rate of 10°C/min. In Situ XRD data obtained at the precision diffractometry-2 station (SSRTC, Novosibirsk) at a wavelength of 0.101 nm.

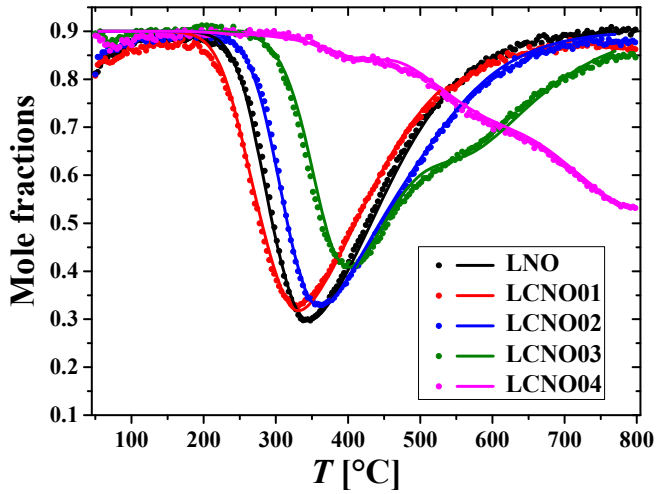

Figure S8. Temperature-programmed isotope exchange of oxygen with $C^{18}O_2$ in the flow reactor for $La_{2-x}Ca_xNiO_{4+\delta}$. Points—experiment, lines—modeling.

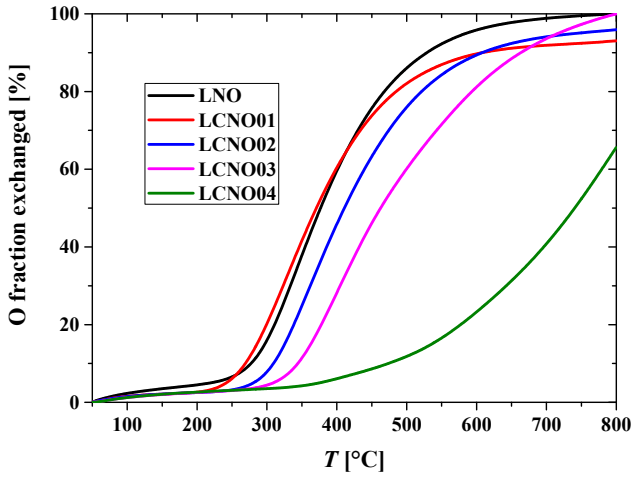

Figure S9. The oxygen fraction exchanged during the TPIE run.

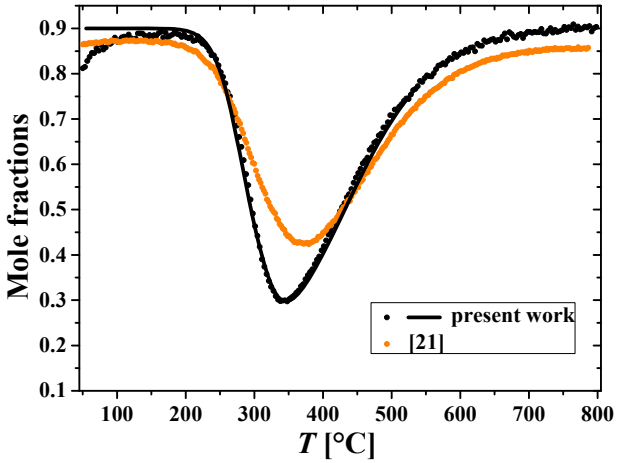

Figure S10. Temperature programmed isotope exchange of oxygen with $C^{18}O_2$ in the flow reactor for $La_2NiO_{4+\delta}$. Points—experiment, lines—modelling.

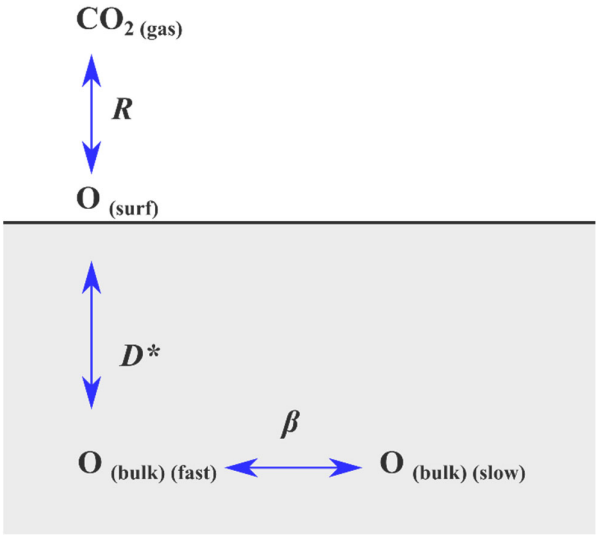

Figure S11. Schematic illustration for mathematical model of oxygen isotope exchange with $C^{18}O_2$ in the flow reactor for Ca-doped La nickelates [29].

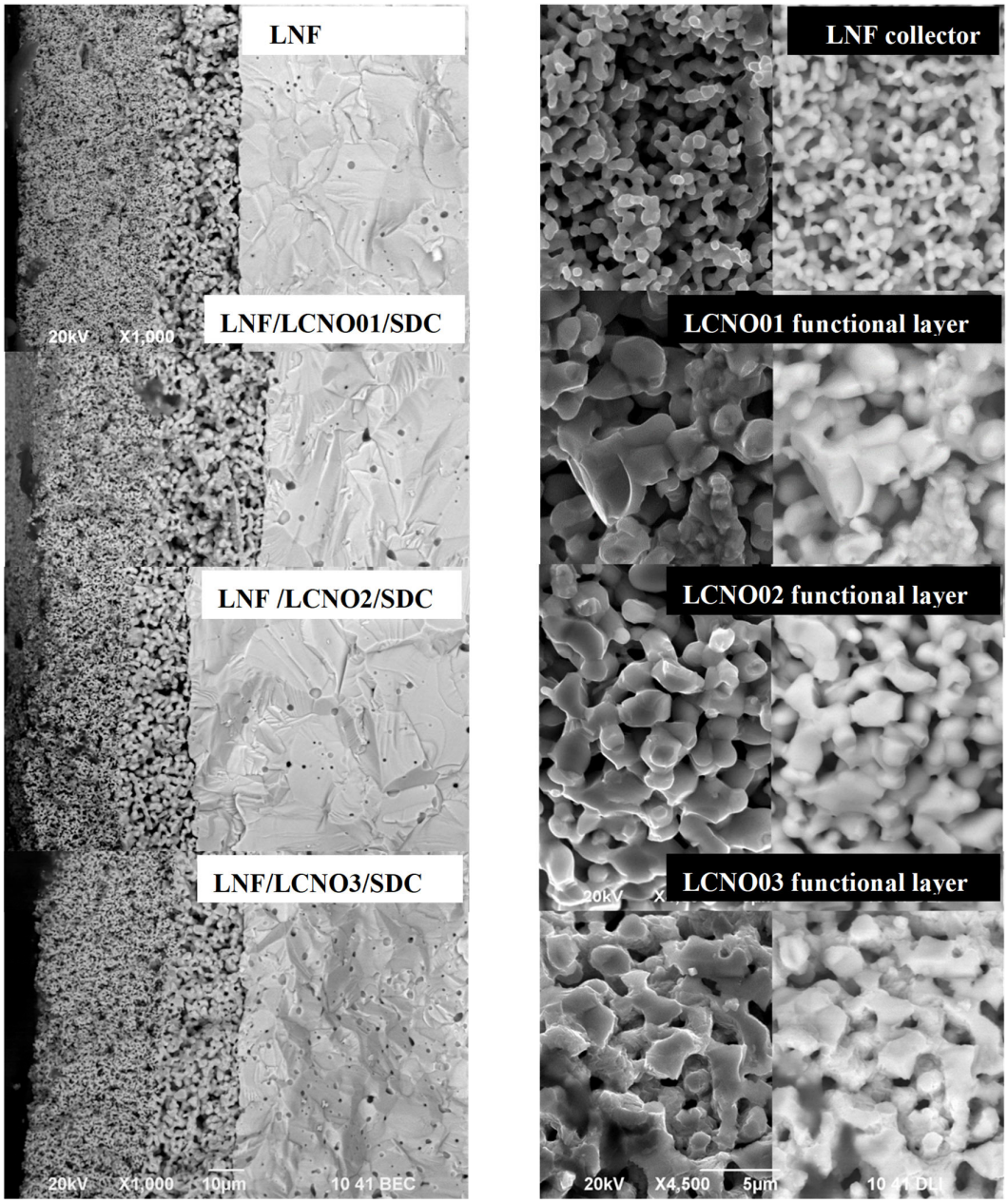

Figure S12. Microstructure of the LNF/LCNO electrodes on the SDC substrate. (T_{sint} = 1250 °C) (left column of images, × 1500); SEM images of the $LaNi_{0.6}Fe_{0.4}O_3$ (LNF) collector and $La_{2-x}Ca_xNiO_{4+\delta}$ (LCNO) functional layers (right column of images, × 4500).

Table S3. Average particle size (<*d*>) of LCNO electrodes.

Sample	Composition	<*d*>, [μm]
LNO	$La_2NiO_{4+\delta}$	0.51
LCNO01	$La_{1.9}Ca_{0.1}NiO_{4+\delta}$	0.57
LCNO02	$La_{1.8}Ca_{0.2}NiO_{4+\delta}$	0.94
LCNO03	$La_{1.7}Ca_{0.3}NiO_{4+\delta}$	0.76